PIER M

(Received 6 September 2023, Accepted 29 November 2023, Scheduled 12 December 2023)

Ultra-Wideband Antenna with Quintuple Band Notches Integrated with Metamaterials

Sapna Arora[1, 2, *], Sharad Sharma[1], and Rohit Anand[3]

[1] *MM(DU), Mullana — Ambala, Haryana, India*
[2] *Panipat Institute of Engineering & Technology Haryana, India*
[3] *Rohit Anand, G.B.Pant DSEU Okhla-1 Campus (formerly GBPEC), New Delhi, India*

ABSTRACT: An elliptical monopole planar antenna for ultra-wideband (UWB) with penta-band-notched characteristics is presented. The frequency band rejection at 3.7 GHz to 4.2 GHz for C-band satellite communication and 5.15 GHz to 5.35 GHz for lower wireless local area network (WLAN) is achieved by etching two elliptical split ring resonators (ESRRs) in the radiating patch. Dual notches at INSAT (4.5 GHz–4.7 GHz) and upper WLAN band (5.725 GHz–5.825 GHz) are created by special type of metamaterial, i.e., a two via double slot type EBG structure. Then, ITU band (7.95 GHz–8.55 GHz) is suppressed by adding a step impedance resonator (SIR) near the feed line. The proposed antenna is designed over a low cost FR4 material substrate, has a miniaturized size of $0.317\lambda \times 0.317\lambda \times 0.007\lambda$, and possesses the impedance bandwidth from 2.5 GHz to 11 GHz. The band notch behaviour of antenna at specific frequencies is explained by mathematical model and justified with numerically simulated surface current distribution and impedance plot. Constant gain with the peak value of 3 dB is measured for UWB except notch bands. Also, this antenna has application in S (1.97–2.69 GHz), LTE (450 MHz–3.8 GHz), C (3.4–7.025 GHz), X (7.25–8.44 GHz), Ku (10.7–14.5 GHz) bands. The proposed antenna structure is a promising candidate for wireless technology.

1. INTRODUCTION

Nowadays, ultra-wideband (UWB) technology is being utilized for numerous wireless applications because of high data rate transmission, low cost, low emission power, low power spectral density, and high resistance to multipath environment systems. Ultra-wideband systems are used for many applications such as medical imaging, wireless body area networks (WBAN), radar systems, military applications, internet of things (IOT), and many others communications [1–4]. For UWB systems, the main requirement for antenna is omnidirectional radiation pattern and broad impedance bandwidth [5, 6]. The monopole antennas with planar structures are a suitable candidate for UWB systems due to small size, ease of integration with planar circuits, low cost, and light weight.

In 2002, Federal Communications Systems allocated the bandwidth from 3.1 GHz to 10.6 GHz for commercial purposes [7]. Several narrow bands share the UWB spectrum that can cause interference in UWB applications. Some of the common narrow band systems in UWB range are WiMAX (IEEE 802.16) operating at 3.3–3.7 GHz, WLAN (IEEE 802.11) at 5.15–5.35 GHz and 5.725–5.825 GHz bands, C band for satellite communications having 3.77–4.2 GHz downlink, 5.9–6.4 GHz uplink band at 7.2–7.65 GHz, and ITU frequency band at 7.95–8.55 GHz. So, in the current research work a miniaturized UWB antenna with multiple filters for suppressing interference with existing narrow band systems to boost the performance of UWB systems is presented.

To achieve band filtering action in UWB antenna, several methods have been proposed in literature. The slots of different shapes (e.g., U-shaped, fork-shaped, L-shaped, E-shaped or circular slots) and sizes have been cut in patch and ground plane to obtain the filtering characteristics at desired frequencies [8–14]. In [15], nonuniform width slots are incorporated in rectangular patch to obtain tri-notches at 3.5 GHz, 5.5 GHz, and 8.1 GHz. By varying the dimensions of slots, center frequencies can be controlled. A compact coplanar waveguide (CPW)-fed antenna is designed by creating a stub having T-shape, a C-shape slot in a circular radiating patch and two L-shaped slots etched in ground plane to introduce notches at WiMAX band, WLAN band, and X-band [16]. A UWB design with U-shaped slots etched on a circular patch to introduce four notch bands and to attain wide bandwidth from 2.9 GHz to 20 GHz is met by creating a rectangular notch in partial ground plane [17]. A beveled rectangle-shaped monopole antenna is proposed in [18] which exhibits a semicircular slot and L-shaped slots on patch to notch X-band and WiMAX band. Also, a semicircular stub is introduced on the opposite side of substrate which is connected to patch with cylindrical pins to suppress WiMAX band.

2. RESEARCH GAPS AND PROPOSED WORK

Electromagnetic band gap (EBG) structures which are a special class of metamaterial are used in antenna design for creating band notch structures [19–21] and providing isolation in MIMO structures [22]. These metamaterials possess unique band gap feature and high impedance at their resonant fre-

* Corresponding author: Sapna Arora (sapnaarora1@gmail.com).

quency. The EBG structure when being placed near the feed line of antenna acts as a band-stop filter, and its band gap property can be utilized in a better way to create notch bands. UWB monopole designs presented in [23–27] exhibit mushroom type EBG structures having a notch bandwidth controlling feature to create notch bands. A single notch for upper WLAN band (5.725 GHz–5.825 GHz) is created in a monopole UWB antenna using a compact two via EBG structure near the feed line [28]. Dual notches are created in [29] by inverted pi notch and spiral shaped EBG structures. However, in above referenced designs one EBG element is able to suppress only single notch.

In the proposed design, a two via double-slot-type EBG (TVDS-EBG) structure is used due to which dual notches are obtained because of two via present in one cell which saves space. Also a limited research work related to UWB antenna with penta notch is available. In the proposed work, an elliptical monopole UWB patch antenna with quintuple notches is presented. The antenna has two elliptical split ring resonators (ESRRs) in radiation patch, one compact dual band EBG structure, and a stepped impedance resonator (SIR) present near the feed line to create penta-notched band simultaneously. The ESRRs created in patch are responsible for creating two notches at C band satellite downlink (3.7 GHz–4.2 GHz) and lower WLAN band (5.15 GHz–5.35 GHz). Dual notches at INSAT (4.5 GHz-4.7 GHz) and upper WLAN band (5.725 GHz–5.825 GHz) are created by one compact dual band EBG structure whereas ITU band (7.95 GHz–8.55 GHz) is suppressed with SIR present near feed line. Therefore, the proposed structure is capable of suppressing five notch bands present in UWB range. High frequency simulation software (HFSS) is used to design and numerically simulate the antenna.

Paper is organized as follows. Section 3 presents the design topology and dimensional parameters. The detailed process of attaining multiple band notches and design evaluation is also explained in this section. Section 4 briefs the reflection coefficient analysis for varying design topologies, parametric analysis, and different substrate materials, surface current distribution, and antenna impedance. Further in Section 5, measured result analysis is presented in terms of reflection coefficient, radiation pattern and gain which is followed by the conclusion in next section.

3. PROPOSED DESIGN

The front and back views of the antenna are shown in Figure 1. To attain the UWB spectrum, an elliptical patch having major axis length $E1$ and minor axis length $E2$ is designed on the top side of substrate and a partial ground plane on the bottom side of substrate. This design is made on the substrate material of FR4 epoxy material having 0.8 mm thickness with dielectric constant, $\varepsilon_r = 4.4$ and loss tangent 0.02. In partial ground plane, the slot is embedded with dimensions $2.5 \times 1.5\,\text{mm}^2$ to increase the impedance bandwidth (2.5 GHz–11 GHz) of design. To feed the radiating patch a 50-ohm microstrip line having length Lf and width Wf is used. In Table 1, the optimized dimensions of proposed design are listed.

TABLE 1. Optimized dimensions of proposed penta-notch UWB antenna.

Parameter	Value (mm)	Parameter	Value (mm)
L	38	$W7$	0.5
W	38	$W8$	0.75
$W1$	4.34	G	1
$L1$	9.6	D	0.2
$L2$	7.54	$L3$	1.58
$W2$	3.278	$L4$	2.19
$D1$	0.5	$L5$	6.42
$D2$	0.5	$W9$	0.15
$D3$	0.33	$K1$	2.22
$D4$	0.27	$K2$	2.3
$E1$	9.95	$W10$	0.15
$E2$	9.63	Wf	1.5
$W3$	11	Lf	18.08
$W4$	8	Lg	18
$W5$	4.5	Ls	1.5
$W6$	1	Ws	2.5

3.1. UWB Monopole Antenna Design Procedure

Figure 2 illustrates the step by step procedure of proposed design. Firstly, an elliptical patch is designed on partial ground plane with a slot to obtain UWB bandwidth as shown in Figure 2(a). The proposed design was simulated on different dielectric materials to achieve the maximum impedance bandwidth. Various dielectrics used for simulation were FR-4 with $\varepsilon_r = 4.4$ and loss tangent 0.02, RT Duroid with $\varepsilon_r = 2.2$ and loss tangent 0.0009, Rogers RO3003 with $\varepsilon_r = 3$ and loss tangent 0.0013, Teflon with $\varepsilon_r = 2.1$ and loss tangent 0.001.

The reflection coefficient graph in Figure 3 depicts that the bandwidth achieved for FR-4 for $S_{11} < -10$ dB ranges from 3.1 GHz–28.03 GHz, for RT Duroid 5880 is 3.09 GHz–19.326 GHz, for Rogers RO3003 is 1 GHz–16.42 GHz, and for Teflon is 3.178 GHz–19.524 GHz. As observed, the bandwidth achieved for FR-4 is the widest which can be employed for applications beyond UWB range, hence FR4 is preferred for the proposed work.

Further steps illustrate the techniques to obtain notches at different frequencies. In Design 2, an elliptical slot is cut from radiating patch to obtain a notch at C-band (3.7 GHz–4.2 GHz) as shown in Figure 2(b). To obtain dual notches at INSAT (4.5 GHz–4.7 GHz) and upper WLAN band (5.725–5.825 GHz), TVDS-EBG is fabricated near feed line as shown in Figure 2(c). An additional notch at (7.95 GHz–8.55 GHz) band is created with SIR as shown in Figure 2(d). Thus, to obtain five notches, one more elliptical slot is created on patch as shown in Figure 2(e) which creates a notch at lower WLAN band (5.15 GHz–5.35 GHz).

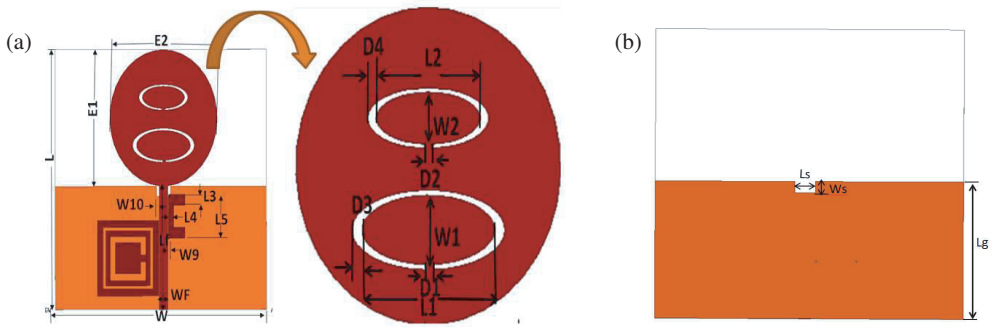

FIGURE 1. Proposed antenna design. (a) Front view. (b) Back view.

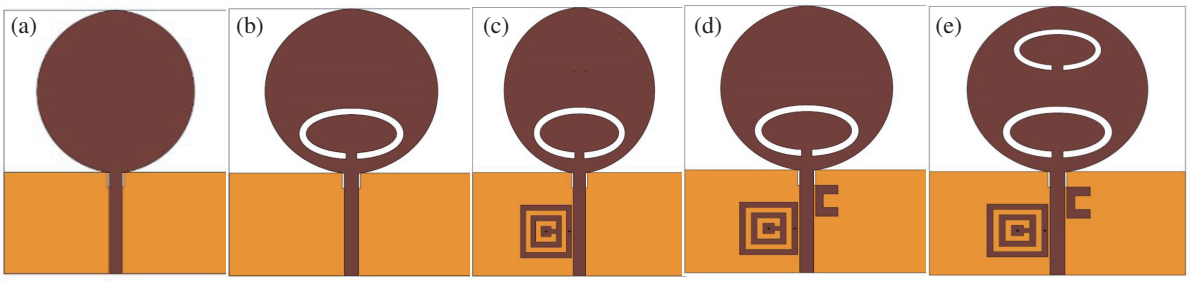

FIGURE 2. Design procedure. (a) Design 1. (b) Design 2. (c) Design 3. (d) Design 4. (e) Proposed Design.

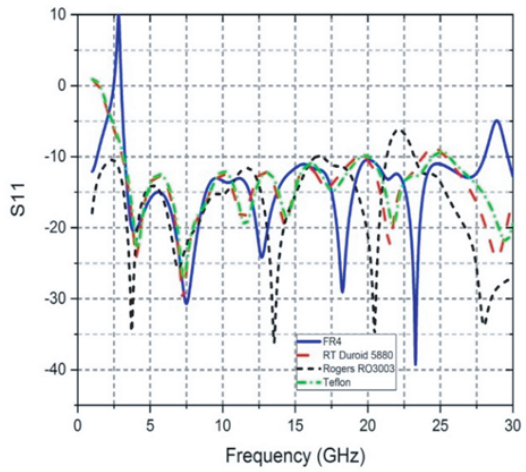

FIGURE 3. $|S_{11}|$ graph depicting performance of various dielectrics on UWB antenna performance.

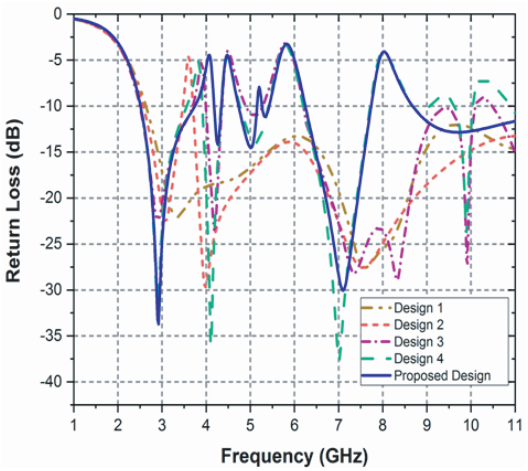

FIGURE 4. Simulated graphs for return loss of Design 1, Design 2, Design 3, Design 4 and proposed design.

The return loss graph for Design 1, Design 2, Design 3, Design 4, and proposed design is shown in Figure 4. The graph shown for Design 1 depicts S_{11} having value less than -10 dB from 2.5 GHz to 11 GHz which satisfies UWB criteria.

3.2. Techniques to Create Notches

At the desired notch bands surface current is confined at the specific parts of the location by etching the elliptical slots and EBG structures. In this design, five bands have been rejected using different techniques as discussed below.

3.3. Band and Lower WLAN Band Rejection

To achieve notches at C-band and lower WLAN band, two elliptical split ring resonators (ESRRs) are etched in patch shown in Figures 2(a) and 2(e). The following Equations are used to find dimensions of ESRR at the notch frequency [30].

$$Ci = \frac{c}{2 * f_{notch}\sqrt{\varepsilon_{eff}}} = K\pi$$

(0.5 minor axis length-width of ESRR) (1)

$$K = 3(1+k) - \sqrt{(3+k)(1+3k)} \tag{2}$$

$$\epsilon_{eff} = \frac{\varepsilon_r + 1}{2} + \frac{\frac{\varepsilon_r - 1}{2}}{\sqrt{1 + \frac{12h}{Wf}}} \tag{3}$$

Here, Ci is the inner circumference of ESRR which must be nearly equal to half of guided wavelength at notch frequency f_{notch}. The factor k is ellipticity (major axis length/minor axis length) related to K through Equation (2). Here K is a factor used to find the inner circumference of ellipse. The effective dielectric constant ε_{eff} is calculated by Equation (3); Wf is the width of micro strip line; 'h' is the height of substrate; and λ_g is the guided wavelength.

The notch at C-band is created by ESRR present in the lower portion of patch having major axis length $L1$, minor axis length $W1$, ellipticity $k1$, and width of cut $D1$. The current distribution at 4.02 GHz is concentrated at lower ESRR which blocks the eradiation outside this region (discussed in next section). The calculated value of Ci from above Equations is 11.5 mm while the optimized value is 11.65 mm which provides a notch at C-band. In Figure 5, the parametric analysis of $D1$ parameter is shown. As the value of $D1$ (gap between two edges of ESRR) increases, the notch shifts from 3.55 mm to 3.7 mm. The optimum value is chosen for $D1 = 0.5$, which provides notch from 3.7–4.12 GHz. The major axis length of the ESRR present in upper portion of radiating patch is $L2$; minor axis length is $W2$; ellipticity $k2$ and width of cut is $D4$, which create a notch at lower WLAN. The calculated value of Ci in this case is 8.69 mm whereas the optimized one is 8.232 mm.

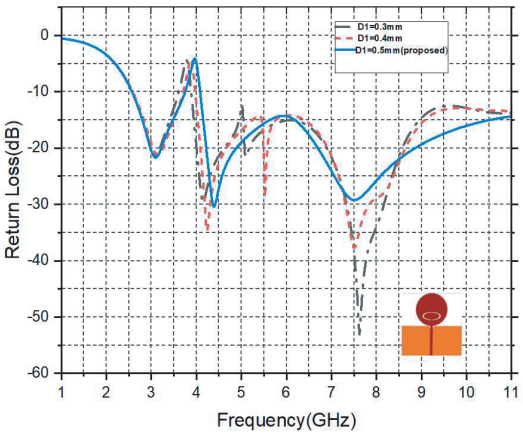

FIGURE 5. Simulated graphs for return loss showing parametric variation of $D1$ parameter.

In reference to Design-2 of Figure 2(a), first ESRR is etched in patch near the feed point. It causes band-stop characteristics for C band satellite down link channel. The curve for Design-2 in Figure 4 shows that S_{11} value is more than -10 dB from 3.7 GHz to 4.12 GHz with the center notch frequency of 3.91 GHz that confirms the first notch at C band and that the remaining UWB spectrum has stable impedance characteristics.

3.3.1. INSAT and Upper WLAN Band Rejection

EBGs are a special class of metamaterial which has unique band gap property. This property is utilized in antenna design to reject unwanted bands. A two via double slot (TVDS) type EBG structure [31] is designed near the feed line to reject the INSAT band and upper WLAN band. The topology of modified antenna (Design-2) is shown in Figure 2(c). Geometry of the EBG structure is shown in Figure 6(a). The diameter of shorting via of the inner square patch having side $W5$ is D. The distance between inner patch and outer slot is $W7$; outer slot width is $W6$; and inner patch width is $W5$.

The gap between the microstrip line and EBG structure is $W10$. TVDS-EBG structure is able to produce two notches because of two series resonant circuit in single cell. The equivalent circuit is shown in Figure 6(b), and inductance ($L1$) is present due to current flowing between via located on edge, ground and via present in inner patch. Capacitance ($C1$) is between outer slot and inner patch with gap $W7$. The capacitance $C1$ and inductance $L1$ constitute the first resonant circuit. The capacitance $C2$ is present between inner slot and inner patch; $C4$ capacitance is due to the gap between adjacent EBG cells; and capacitance $C3$ is present due to the gap between outer slot and inner patch. The inductance $L2$ is due to the current flowing from edge located via to centre located via of an adjacent EBG cell. The capacitances $C2$, $C3$, $C4$ and inductance $L2$ form the second resonant circuit in series with the first one. Dual resonance frequencies of the TVDS-EBG structure can be evaluated by using Equations (4)–(6).

$$F_{c1} = \frac{1}{2 * \pi\sqrt{L1C1}} \tag{4}$$

$$F_{c2} = \frac{1}{2\pi\sqrt{L2C_{eq}}} \tag{5}$$

$$\text{Here, } \frac{1}{C_{eq}} = \frac{1}{C2} + \frac{1}{C3} + \frac{1}{C4} \tag{6}$$

To find the values of passive components ($L1$, $C1$, $L2$, $C2$, $C3$, and $C4$), the equivalent circuit of EBG was simulated in ADS schematic environment as shown in Figure 6(c). With the help of tuning feature in ADS different parameters' values were obtained to match the simulated curve of S_{11}. Tables 2(a) & (b) compare the simulated, measured and equivalent circuit notch frequencies.

To validate the band gap properties of TVDS-EBG, a unit cell is simulated in eigen-mode solution of Ansys high-frequency simulator to obtain rectangular irreducible Brillouin-zone based dispersion diagram. The bandgaps are evaluated from dispersion analysis on single cell, and infinite structure is created by imposing periodic boundary condition (PBC) on unit cell in eigen-mode solver of High Frequency Structure Simulator (HFSS). Dispersion diagram for the unit cell is shown in Figure 7, and here frequency is shown on vertical axis. The horizontal axis shows the transverse wave numbers k_x and k_y which represent wave propagation vectors. These vectors in unit cell represent the boundary region of wave propagation which is known as irreducible Brillouin zone. The first mode starts

TABLE 2. Comparison of simulated measured and LC equivalent lumped element notch frequency.

Notch Band	Simulated notched frequency (GHz)	Measured notched frequency (GHz)	frequency measured from LC Equivalent Circuit (GHz)	$L1$ (nH)	$C1$ (pf)
INSAT	4.53	4.5	4.48	0.07	0.18

(a)

Notch Band	Simulated notched frequency (GHz)	Measured notched frequency (GHz)	frequency measured from LC Equivalent Circuit (GHz)	$L2$ (nH)	$C2$ (pf)	$C3$ (pf)	$C4$ (pf)
Upper WLAN	5.84	5.9	5.68	0.11	350	12.2	17.83

(b)

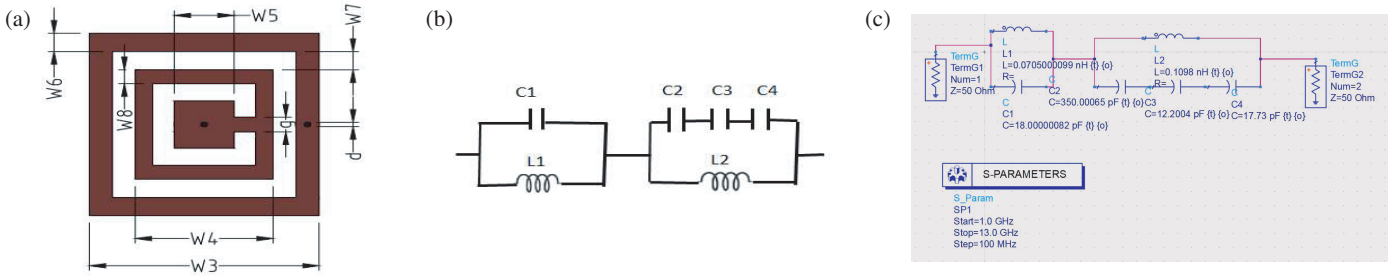

FIGURE 6. (a) TVDS-EBG structure. (b) Equivalent circuit of EBG. (c) Equivalent circuit of EBG in ADS Schematic environment.

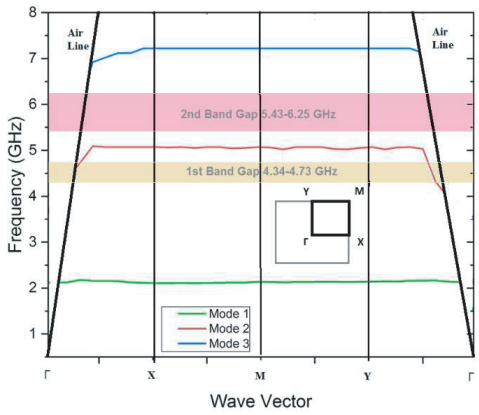

FIGURE 7. Dispersion diagram for TVDS-EBG structure.

at zero frequency, increases with wave number, and reaches 4.73 GHz. The first band gap at 4.34–4.73 GHz between Mode 1 and Mode 2 and second band gap at 5.43–6.25 GHz between mode 2 and mode 3 have been observed. These band gaps tell that no surface waves exist inside this frequency ranges.

The topology of antenna after adding the EBG structure is shown in Figure 2(c). To justify the effect of selected EBG structure, $|S_{11}|$ curve for design-3 is plotted in Figure 4. The second and third notches from 4.34 GHz to 4.73 GHz and at 5.43 to 6.25 GHz band with centre frequencies of 4.53 GHz and 5.84 GHz can be observed, thus creating notches at INSAT and upper WLAN band in addition to notch 1. In Figure 8, the return loss variations of EBG structure with variation in gap $W10$ with feedline are shown.

3.3.2. ITU Band Suppression

To suppress the ITU band at 7.95 GHz to 8.55 GHz, a step impedance resonator [32] is introduced near the feed line at $W9$ distance. The topology for it is shown in Figure 2(d). SIR is a nonuniform transmission line resonator that acts as a band-pass filter. The higher the gap is, the less the coupling will be between resonator and feed line. $L3$ and $L4$ dimensions are set with parametric variation to get notches at desired frequencies.

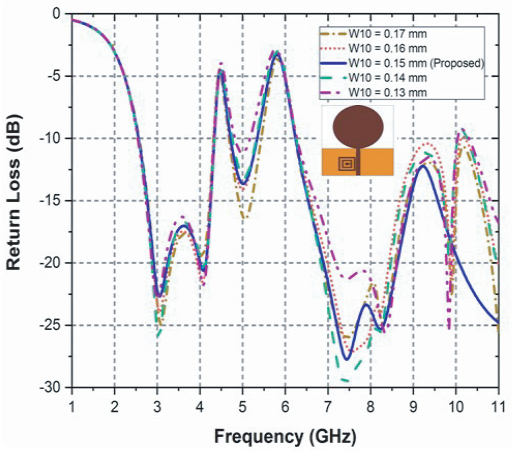

FIGURE 8. Return loss variations of EBG structure with varying gap $W10$ with feed line.

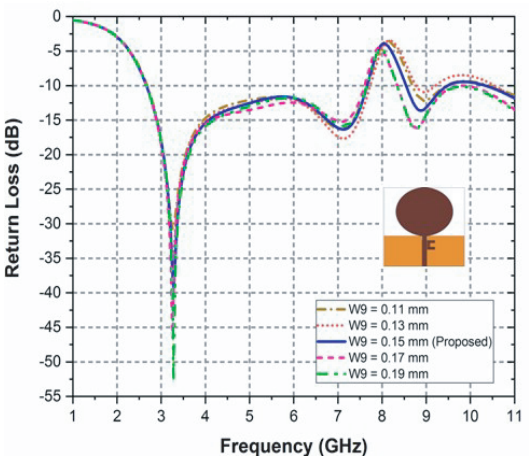

FIGURE 9. Return loss variations of SIR structure with varying gap $W9$ with feed line.

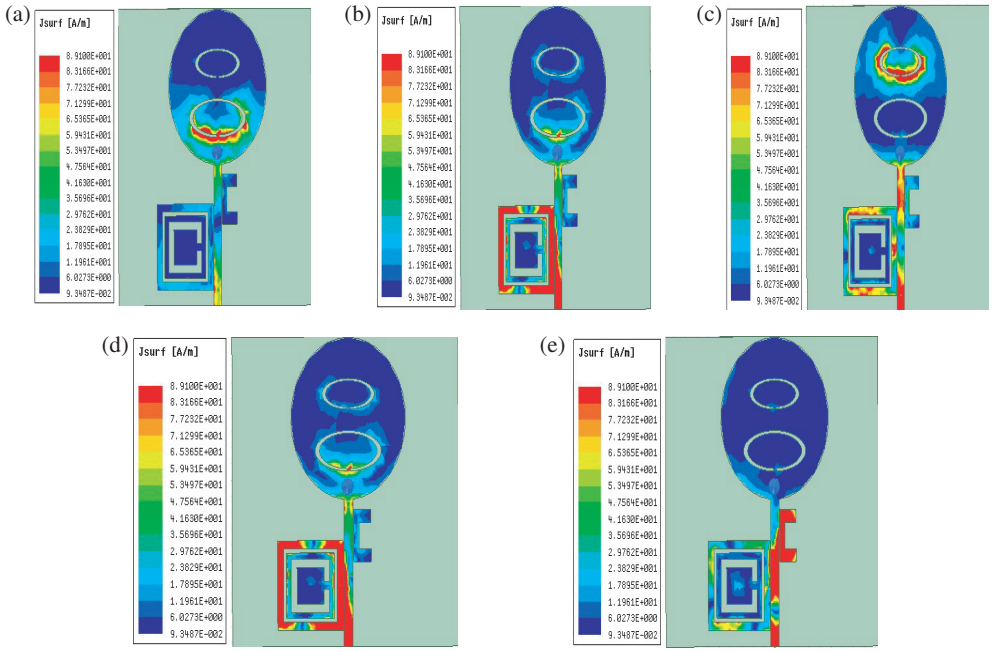

FIGURE 10. Surface current distribution of proposed design at (a) 4.02 GHz, (b) 4.54 GHz, (c) 5.22 GHz, (d) 5.9 GHz, (e) 8.08 GHz.

The design equations for SIR are given by following Equations (7)–(8).

$$\frac{f_{s1}}{f0} = \pi/(2\tan^{-1}\sqrt{K1}) \tag{7}$$

$K1$ is Impedance ratio

$$L5 = \tan^{-1}\sqrt{K1} \tag{8}$$

Here, f_{s1} is the first spurious resonance frequency, and $f0$ is the resonance frequency (8.25 GHz), centre frequency of ITU band. Design 4 curve in Figure 4 depicts the fourth notch at 7.73 GHz–8.69 GHz having a centre frequency of 8.21 GHz in addition to notches 1, 2, and 3.

Finally, Design-4 is altered by etching the second ESRR in the patch as shown in Figure 2(e) which is the proposed structure. It causes the band suppression at lower WLAN band with frequency ranging from 5.15 GHz to 5.26 GHz. In this way, the proposed design is able to produce a penta notch in UWB range. The $|S_{11}|$ plot for proposed structure is shown in Figure 4.

4. SIMULATED RESULTS AND DISCUSSION

In this section, the parametric analysis of antenna, surface current distributions, and impedance curve of proposed design are discussed.

Parametric analysis for the gap between EBG structure and feed line '$W10$' is performed. The reflection coefficient plot for the varying '$W10$' is shown in Figure 7. It is clear from the graph that as the gap increases from 0.13 mm to 0.17 mm

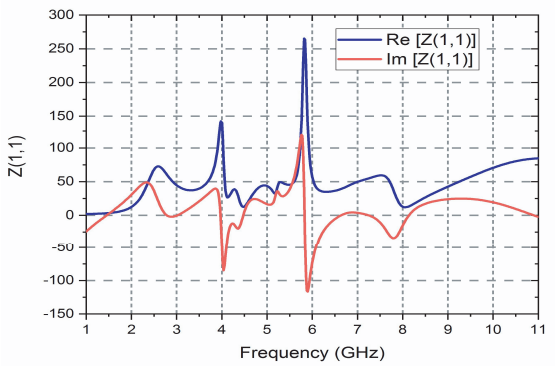

FIGURE 11. Input Impedance of proposed antenna.

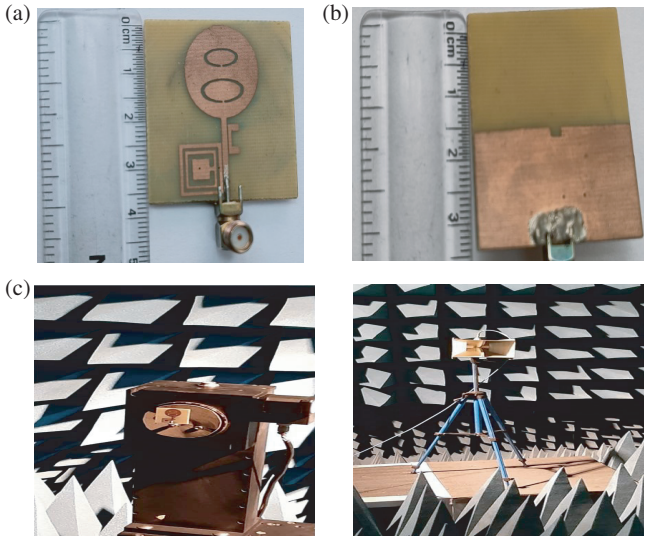

FIGURE 12. (a) Fabricated proposed antenna — Front view. (b) Rear view. (c) Screenshot of measurement in chamber.

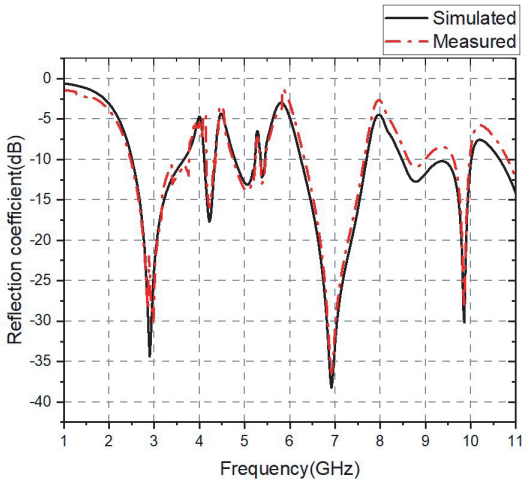

FIGURE 13. Simulated and measured reflection coefficient.

the bandwidth of notches and level of notches decrease. It is due to the reduction in mutual coupling between EBG and feed line. The gap of 0.15 mm provides notches at desired INSAT (4.5 GHz–4.7 GHz) and upper WLAN band (5.725–5.825 GHz) from 4.34 GHz to 4.73 GHz and from 5.43 GHz to 6.25 GHz, respectively.

Another important parametric analysis is performed for the gap between SIR structure and feed line '$W9$'. The reflection coefficient plot for the varying '$W9$' is shown in Figure 9. As the gap is increased from 0.11 mm to 0.19 mm, the level of notches and bandwidth starts diminishing due to th eweak mutual coupling between feed line and SIR. The desired notch at ITU band (7.95 GHz–8.55 GHz) is obtained with a gap of 0.15 mm, so this value is considered for the design.

Further to understand the behaviour of antenna, surface current distribution on radiating patch, EBG structure and SIR is analyzed. The current distribution plot at notched bands is shown in Figure 10. It can be observed that when antenna operates at 3.91 GHz, the current is concentrated on lower ESRR, and no radiation takes place outside ESRR as indicated in Figure 10(a). As frequency is increased, the current concentrates more on EBG structure at 4.53 GHz and 5.84 GHz shown in Figures 10(b) & 10(c), thus reducing the radiation at these frequencies. In Figure 10(d), current concentrates on upper ESRR at 5.20 GHz and at 8.21 GHz current density surrounds SIR as shown in Figure 10(e).

Thus at notched frequencies, current is more intensive at band notched elements, which indicates that more energy is stored around these elements instead of radiation in surroundings. It also confirms the band rejection nature of proposed design at five bands. The input impedance curve of proposed design has been shown in Figure 11. It is clear from the graph that for UWB resistance is near 50 ohm, and reactance is nearly 0 ohm except notches. At the first notch (3.76 GHz–4.10 GHz) and fourth notch (5.5 GHz–6.32 GHz), resistance is very high (140 ohms and 270 ohm), and reactance is negative that is similar to parallel RLC circuit.

However, resistance is less than 50 ohms at the second notch (4.42 GHz–4.74 GHz), third notch (5.17 GHz to 5.27 GHz), and fifth notch (7.76 GHz to 8.88 GHz) whereas reactance is positive that resembles series resonance circuit.

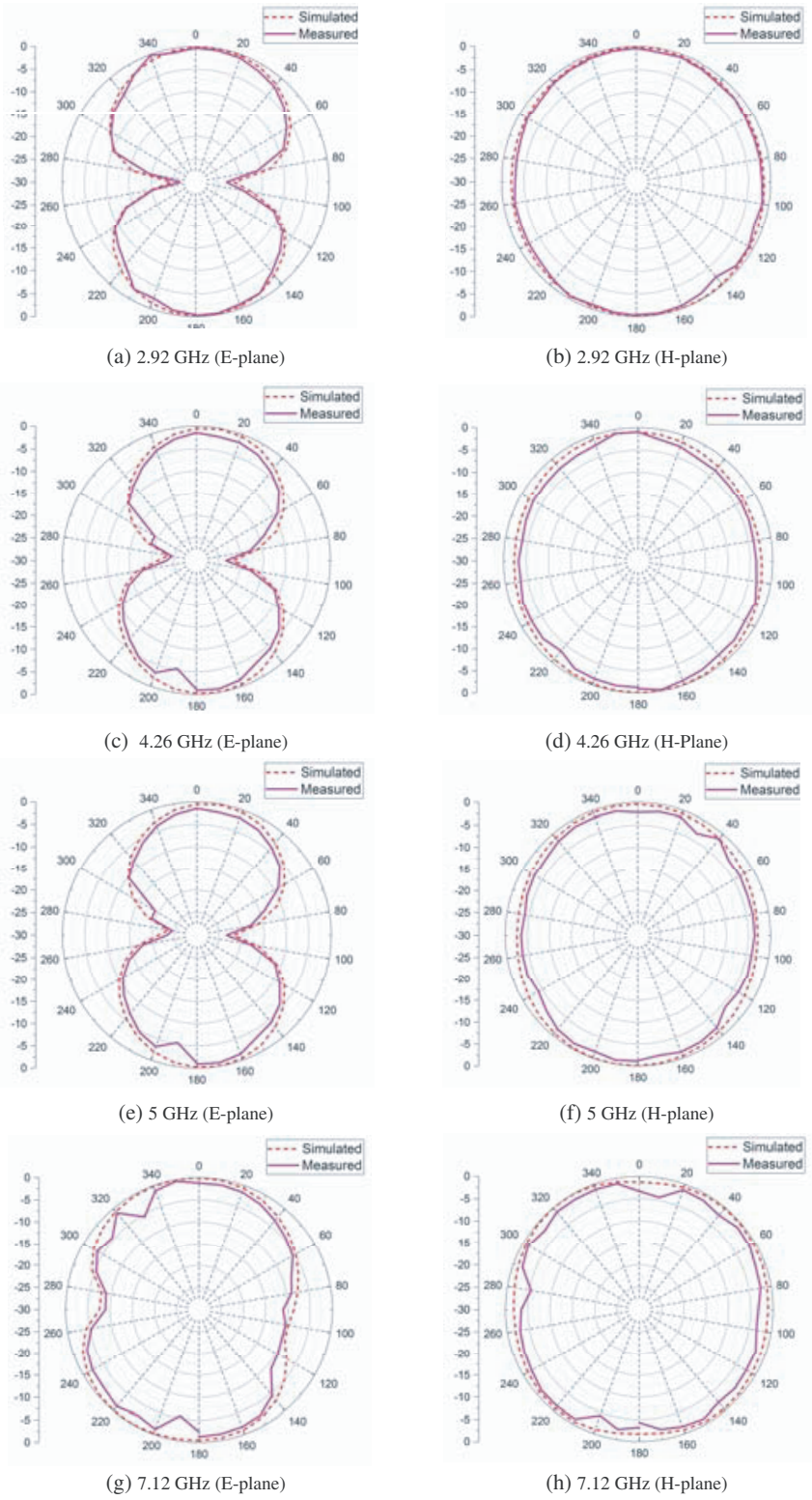

(a) 2.92 GHz (E-plane)
(b) 2.92 GHz (H-plane)
(c) 4.26 GHz (E-plane)
(d) 4.26 GHz (H-Plane)
(e) 5 GHz (E-plane)
(f) 5 GHz (H-plane)
(g) 7.12 GHz (E-plane)
(h) 7.12 GHz (H-plane)

FIGURE 14. Comparison of measured and simulated radiation patterns: (a) (b) at 2.92 GHz; (c) (d) at 4.26 GHz; (e) (f) at 5 GHz; (g) (h) at 7.12 GHz.

5. EXPERIMENTAL ANALYSIS

The front and rear views of fabricated design and screenshot in experimental analysis are shown in Figure 12. To measure return loss graph, vector network analyser has been used, and radiation characteristics are computed in an anechoic chamber. The simulated and measured graphs for reflection coefficient for the proposed design are plotted in Figure 13. It has been found that S_{11} value is more than -10 dB at five notched bands and lower than -10 dB for rest of frequencies from 2.5 GHz to 11 GHz. The simulated and measured S_{11} results are in fair agreement with each other except a small deviation towards

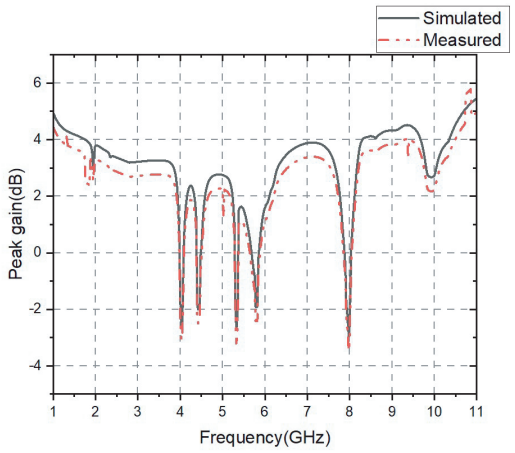

FIGURE 15. Simulated and measured peak gain comparison.

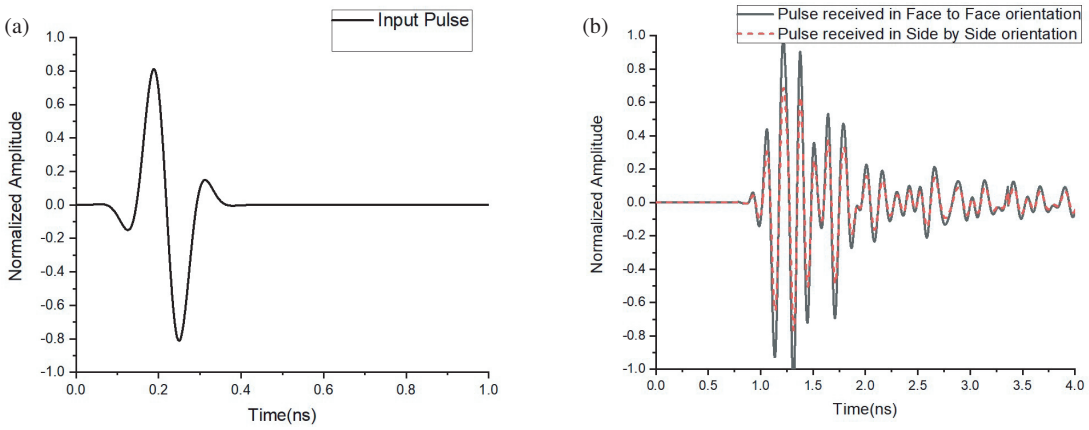

FIGURE 16. Transient time domain analysis of proposed notched-band antenna. (a) Input pulse. (b) Received pulses.

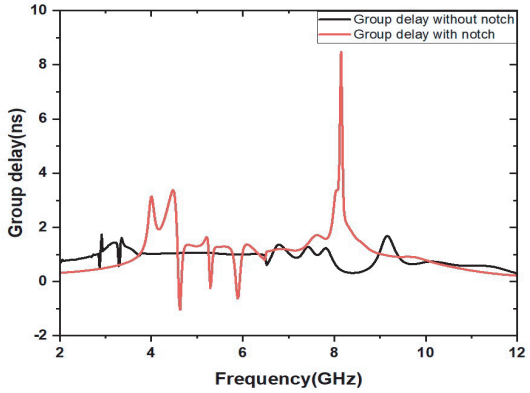

FIGURE 17. Group delay without and with notch bands.

lower frequency that may be due to soldering temperature and tolerances [33]. The antenna has presented excellent response for the desired UWB frequency range with notch band featured at five communication standards. It makes antenna suitable for UWB communication without the interference with other narrow band standards.

The plots of radiation patterns for the proposed design at frequencies of 2.92 GHz, 4.26 GHz, 5 GHz, and 7.12 GHz are measured in both E- and H-planes and compared with simulated one in Figures 14(a), 14(b), 14(c), and 14(d), respectively. In H-plane, an omnidirectional radiation pattern and in E-plane, a dipole like radiation pattern are observed for both measured and simulated counterparts. The measured radiation patterns and simulated ones are nearly matched except at 7.12 GHz where a slight mismatch is observed, which can be

TABLE 3. Comparison of the proposed antenna with existing antennas.

Ref.	Overall size (mm^3)	Bandwidth of operation (GHz)	No. of notches	Notched frequency band (GHz)
[36]	$38 \times 44 \times 0.8$ (= 1337.6)	3.1–10.6	2	(4.96–5.42), (5.71–5.91)
[37]	$35 \times 44 \times 1$ (= 1540)	2–12	4	(3.39–3.88), (5.11–5.97), (8.0–8.71)
[38]	$80 \times 80 \times 0.508$ (= 3251.2)	2.2–11	5	(1.85–2.49), (2.91–3.49), (5.65–6.25), (7.19–8.78)
[39]	$36 \times 38 \times 1.6$ (= 2188.8)	2.86–13.3	5	(3.45–4), (5.15–5.9), (6.77–8), (8.3–9.1), (9.3–10.6)
[40]	$26 \times 31.8 \times 1.6$ (= 1322.8)	2.45–12	5	(3.27–3.57), (5.01–5.45), (5.55–6.05), (7.05–7.45), (7.83–8.19)
[41]	$31 \times 25 \times 1.6$ (= 1240)	3.05–10.6	5	(3.4–3.8), (5.1–5.35), (5.6–6), (7.15–7.65), (8.05–8.65)
[42]	$31.3 \times 34.9 \times 1.6$ (= 1747.7)	2.9–10.5	5	(2.4–2.9), (3.6–4.3), (5.3–5.7), (6.4–6.7), (7.8–8.6)
Proposed design	$38 \times 38 \times 0.8$ (= 1155.2)	2.5–11	5	(3.7–4.12), (4.34–4.73), (5.43–6.25), (7.73–8.69), (5.15–5.26)

due to enhanced dielectric loss in FR4 substrate with increase in frequency.

In Figure 15, measured and simulated peak gains have good agreement as shown with a maximum gain of 3 dB at 9.5 GHz and 2.5 dB at 9.3 GHz, respectively. The peak gain decreases at 3.91 GHz, 4.53 GHz, 5.2 GHz, 5.84 GHz, 8.21 GHz which clearly shows the quintuple notch created by the proposed antenna and remains greater than 2 dB for rest of the frequencies in UWB.

To find pulse handling capability of the proposed design, time domain analysis has been performed with transient solution type feature and group delay [34–36]. An impulse waveform is applied as input signal according to Federal Communications Commission (FCC) for UWB systems as shown in Figure 15. To perform simulated dispersion, two identical antennas are placed at a distance of 200 mm (greater than far field distance) in side by side and face to face configurations. It is clear from Figures 16 and 17 that notches obtained at centre frequencies (at 3.91 GHz, 4.53 GHz, 5.2 GHz, 5.84 GHz, 8.21 GHz) create more ringing and distortion of pulse. Group delay is measured to check distortion in transmitted pulse. The group delay of proposed design is shown in Figure 17. Here, the value of group delay is less than 2 ns for the whole ultrawide bandwidth for an antenna without notches. At notch bands variation in group delay is more which shows distortion on these frequencies.

In Table 3, the proposed design is compared with reported antennas. The comparison is done on the basis of overall size, bandwidth of operation, number of notches and notched frequency band. In [36], only two bands are notched with a C-shaped slot and stub. Compared to [36, 37], the proposed antenna provides more notches in the entire UWB range in spite of smaller overall dimensions. In [38], time domain analysis has not been shown to check the suitability of design for UWB applications. Designs in [39–42] are comparatively complex in geometry and have larger dimensions than the proposed antenna.

6. CONCLUSIONS

In this paper, a UWB monopole antenna with quintuple notch is presented. Five stopbands at C band satellite downlink (3.7 GHz–4.2 GHz) and lower WLAN band (5.15 GHz–5.35 GHz), INSAT (4.5 GHz–4.7 GHz), upper WLAN band (5.725 GHz–5.825 GHz), ITU band (7.95 GHz–8.55 GHz) are achieved as shown in simulated and measured reflection coefficients. The proposed antenna has dipole like radiation patterns at E-plane and radiation pattern at H-plane with gain greater than 2.5 dB. Moreover, the proposed antenna has a wide impedance bandwidth from 2.5 GHz to 11 GHz and thus a good candidate for UWB systems

REFERENCES

[1] Bekasiewicz, A. and S. Koziel, "Compact UWB monopole antenna for internet of things applications," *Electronics Letters*, Vol. 52, No. 7, 492–493, Apr. 2016.

[2] Allen, B., M. Dohler, E. Okon, W. Malik, A. Brown, and D. Edwards, *Ultra-wideband Antennas and Propagation: For Communications, Radar and Imaging*, John Wiley & Sons, 2006.

[3] Chibber, A., R. Anand, and S. Arora, "A staircase microstrip patch antenna for UWB applications," in *2021 9th International Conference on Reliability, Infocom Technologies and Optimization (Trends and Future Directions) (ICRITO)*, 1–5, 2021.

[4] Adamiuk, G., T. Zwick, and W. Wiesbeck, "UWB antennas for communication systems," *Proceedings of The IEEE*, Vol. 100, No. 7, 2308–2321, Jul. 2012.

[5] Anand, R. and P. Chawla, "Bandwidth optimization of a novel slotted fractal antenna using modified lightning attachment procedure optimization," *Smart Antennas*, 379–392, 2022.

[6] Anand, R. and P. Chawla, "Optimization of inscribed hexagonal fractal slotted microstrip antenna using modified lightning attachment procedure optimization," *International Journal of Microwave and Wireless Technologies*, Vol. 12, No. 6, 519–530, Jul. 2020.

[7] Federal Communications Commission, "Revision of part 15 of the commission's rules regarding ultra-wideband transmission systems," *First Report and Order Fcc 02-48*, 2002.

[8] Marimuthu, J. and M. Esa, "Compact UWB PCML bandpass filter with L- and C-shaped resonator," *Electronics Letters*, Vol. 44, No. 6, 419–421, 2008.

[9] Lu, J.-H. and C.-H. Yeh, "Planar broadband arc-shaped monopole antenna for UWB system," *IEEE Transactions on Antennas and Propagation*, Vol. 60, No. 7, 3091–3095, Jul. 2012.

[10] Yadav, S., A. K. Gautam, and B. K. Kanaujia, "Design of dual band-notched lamp-shaped antenna with UWB characteristics," *International Journal of Microwave and Wireless Technologies*, Vol. 9, No. 2, 395–402, Mar. 2017.

[11] Rahman, M., "CPW fed miniaturized UWB tri-notch antenna with bandwidth enhancement," *Advances in Electrical Engineering*, Vol. 2016, 2016.

[12] Kumar, O. P., P. Kumar, and T. Ali, "A compact dual-band notched UWB antenna for wireless applications," *Micromachines*, Vol. 13, No. 1, 12, Jan. 2022.

[13] Kumar, P., M. M. M. Pai, P. Kumar, T. Ali, M. G. N. Alsath, and V. Suresh, "Characteristics mode analysis-inspired compact UWB antenna with WLAN and X-band notch features for wireless applications," *Journal of Sensor and Actuator Networks*, Vol. 12, No. 3, 37, Jun. 2023.

[14] Arora, S., S. Sharma, R. Anand, and G. Shrivastva, "Miniaturized pentagon-shaped planar monopole antenna for ultra-wideband applications," *Progress In Electromagnetics Research C*, Vol. 133, 195–208, 2023.

[15] Chen, X., F. Xu, and X. Tan, "Design of a compact UWB antenna with triple notched bands using nonuniform width slots," *Journal of Sensors*, Vol. 2017, 1–9, 2017.

[16] Sharma, M., Y. K. Awasthi, and H. Singh, "Design of CPW-fed high rejection triple band-notch UWB antenna on silicon substrate with diverse wireless applications," *Progress In Electromagnetics Research C*, Vol. 74, 19–30, 2017.

[17] Ghimire, J. and D.-Y. Choi, "Design of a compact ultrawideband u-shaped slot etched on a circular patch antenna with notch band characteristics for ultrawideband applications," *International Journal of Antennas and Propagation*, Vol. 2019, 2019.

[18] Emadian, S. R. and J. Ahmadi-Shokouh, "Study on frequency and time domain properties of novel triple band notched UWB antenna in indoor propagation channel," *International Journal of RF and Microwave Computer-aided Engineering*, Vol. 28, No. 9, e21428, Nov. 2018.

[19] Peddakrishna, S. and T. Khan, "Design of UWB monopole antenna with dual notched band characteristics by using π-shaped slot and EBG resonator," *AEU-international Journal of Electronics and Communications*, Vol. 96, 107–112, 2018.

[20] Kollipara, V., S. Peddakrishna, and J. Kumar, "Planar EBG loaded UWB monopole antenna with triple notch characteristics," *International Journal of Engineering and Technology Innovation*, Vol. 11, No. 4, 294–304, Sep. 2021.

[21] Peddakrishna, S., V. Kollipara, J. Kumar, and T. Khan, "Slot and EBG-loaded compact quad band-notched UWB antenna," *Iranian Journal of Science and Technology-transactions of Electrical Engineering*, Vol. 46, No. 1, 205–212, Mar. 2022.

[22] Kumar, J., "Compact MIMO antenna," *Microwave and Optical Technology Letters*, Vol. 58, No. 6, 1294–1298, 2016.

[23] Peng, L. and C.-L. Ruan, "UWB band-notched monopole antenna design using electromagnetic-bandgap structures," *IEEE Transactions on Microwave Theory and Techniques*, Vol. 59, No. 4, 1074–1081, Apr. 2011.

[24] Yazdi, M. and N. Komjani, "Design of a band-notched UWB monopole antenna by means of an EBG structure," *IEEE Antennas and Wireless Propagation Letters*, Vol. 10, 170–173, 2011.

[25] Jaglan, N., B. K. Kanaujia, S. D. Gupta, and S. Srivastava, "Design and development of an efficient EBG structures based band notched UWB circular monopole antenna," *Wireless Personal Communications*, Vol. 96, No. 4, 5757–5783, Oct. 2017.

[26] Liu, H. and Z. Xu, "Design of UWB monopole antenna with dual notched bands using one modified electromagnetic-bandgap structure," *Scientific World Journal*, 2013.

[27] Chen, Z., W. Zhou, and J. Hong, "A miniaturized MIMO antenna with triple band-notched characteristics for UWB applications," *IEEE Access*, Vol. 9, 63 646–63 655, 2021.

[28] Dalal, P. and S. K. Dhull, "Upper WLAN band notched UWB monopole antenna using compact two via slot electromagnetic band gap structure," *Progress In Electromagnetics Research C*, Vol. 100, 161–171, 2020.

[29] Sanmugasundaram, R., S. Natarajan, and R. Rajkumar, "Ultra-wideband notch antenna with EBG structures for WiMAX and satellite application," *Progress In Electromagnetics Research Letters*, Vol. 91, 25–32, 2020.

[30] Choudhary, H., T. Singh, K. A. Ali, A. Vats, P. K. Singh, D. R. Phalswal, and V. Gahlaut, "Design and analysis of triple band-notched micro-strip UWB antenna," *Cogent Engineering*, Vol. 3, No. 1, 1249603, 2016.

[31] Bhavarthe, P. P., S. S. Rathod, and K. T. V. Reddy, "A compact dual band gap electromagnetic band gap structure," *IEEE Transactions on Antennas and Propagation*, Vol. 67, No. 1, 596–600, Jan. 2019.

[32] Xiao, J.-K., S.-W. Ma, and Y. Li, "A compact microstrip stepped-impedance resonator and filter," *Microwave Journal*, Vol. 50, No. 2, 116+, Feb. 2007.

[33] Dahiya, A., R. Anand, N. Sindhwani, and D. Kumar, "A novel multi-band high-gain slotted fractal antenna using various substrates for X-band and Ku-band applications," *Mapan-Journal of Metrology Society of India*, Vol. 37, No. 1, 175–183, Mar. 2022.

[34] Sharma, M., "Superwideband triple notch monopole antenna for multiple wireless applications," *Wireless Personal Communications*, Vol. 104, No. 1, 459–470, Jan. 2019.

[35] Sharma, M., Y. K. Awasthi, H. Singh, R. Kumar, and S. Kumari, "Design of compact flower shape dual notched-band monopole antenna for extended UWB wireless applications," *Frequenz*, Vol. 70, No. 11–12, 499–506, Nov. 2016.

[36] Dong, D., S. Chen, Z. Liao, and G. Liu, "A CPW-fed dual-band-notched antenna with sharp skirt selectivity for UWB applications," *International Journal of Antennas and Propagation*, Vol. 2014, 2014.

[37] Li, T., H. Zhai, G. Li, L. Li, and C. Liang, "A compact ultra-wideband antenna with four band-notched characteristics," *Microwave and Optical Technology Letters*, Vol. 54, No. 12, 2862–2865, Dec. 2012.

[38] Liu, J. J., K. P. Esselle, S. G. Hay, and S. S. Zhong, "Planar ultra-wideband antenna with five notched stop bands," *Electronics Letters*, Vol. 49, No. 9, 579–580, Apr. 2013.

[39] Mewara, H. S., J. K. Deegwal, and M. M. Sharma, "A slot resonators based quintuple band-notched Y-shaped planar monopole ultra-wideband antenna," *AEU-International Journal of Electronics and Communications*, Vol. 83, 470–478, 2018.

[40] Xu, J., D. Shen, X. Zhang, and K. Wu, "A compact disc ultrawideband (UWB) antenna with quintuple band rejections," *IEEE Antennas and Wireless Propagation Letters*, Vol. 11, 1517–1520, 2012.

[41] Islam, M. M., M. T. Islam, M. Samsuzzaman, and M. R. I. Faruque, "Five band-notched ultrawide band (UWB) antenna loaded with C-shaped slots," *Microwave and Optical Technology Letters*, Vol. 57, No. 6, 1470–1475, 2015.

[42] Modak, S., T. Khan, and R. H. Laskar, "Penta-notched UWB monopole antenna using EBG structures and fork-shaped slots," *Radio Science*, Vol. 55, No. 9, 1–11, Sep. 2020.